Terahertz pulse shaping via optical rectification in poled lithium niobate

Y.-S. Lee,[a] N. Amer, and W. C. Hurlbut
Department of Physics, Oregon State University, Corvallis, Oregon 97331

(Received 3 September 2002; accepted 13 November 2002)

We demonstrate a technique for terahertz pulse shaping via optical rectification in the pre-engineered domain structure of poled lithium niobate crystals. The terahertz wave forms coincide with the crystal domain structures. The one-dimensional nonlinear wave equation simulates the experimental results with a good qualitative agreement. © *2003 American Institute of Physics.* [DOI: 10.1063/1.1535268]

Terahertz (THz) regime is the most recently explored frequency range in the spectrum of electromagnetic radiation. Femtosecond laser technology has been exploited in the development of THz sources and detectors.[1–5] The detection schemes resolve THz wave forms in time domain with femtosecond resolution, giving rise to THz time-domain spectroscopy (THz–TDS). Many resonances of molecular dynamics in the THz regime were accessible before only by indirect probing methods such as Raman spectroscopy; THz spectroscopy finally makes it possible to directly probe the previously inaccessible resonances. THz–TDS has been applied to gas-phase rotational dynamics,[6,7] carrier dynamics, and intermolecular dynamics in liquids,[8,9] dielectric response of molecules, and polymers.[10,11] In these applications, single-cycle THz waves were used. Since single-cycle THz waves intrinsically possess a broad bandwidth, they are particularly useful for investigating the THz response of matter over a wide range of spectrum simultaneously. In many applications, however, arbitrary THz wave form generators will greatly extend the scope of the THz spectroscopy, in analogy with the user specified wave forms used in optical pulse shaping, or the rf wave forms used in nuclear magnetic resonance. For example, THz–TDS with shaped THz pulses can be applied to the investigation of quantum coherence and nonlinear response of the molecular resonances by manipulating and monitoring temporal evolution of the quantum transitions. Precise control and manipulation of quantum systems is essential to quantum information processes; the THz pulse shaping technique will make it possible to coherently and arbitrarily control quantum wave packets of the molecular resonances. Furthermore, shaped THz pulses are applicable to coherent control of phonon modes in solids, rotational and vibrational mode spectroscopy on surfaces, ultrafast carrier dynamics in semiconducting nanostructures, among other applications.

In this letter, we demonstrate a technique to shape THz pulses using the pre-engineered domain structure of poled lithium niobate (PLN) crystals. The THz pulse shaping technique utilizes a second order nonlinear optical response (optical rectification in nonlinear crystals) and works directly in the time domain. A preliminary THz pulse shaping has been demonstrated by generating simple narrow-band THz wave forms in periodically poled lithium niobate (PPLN).[12–14] The concept of the technique can be extended to generate complicated THz wave forms in more complex domain structures. The domain structure of a PPLN crystal has been quantitatively mapped by analyzing THz wave forms from the crystal.[15] The THz wave form analysis reproduces root-mean-square domain width fluctuations with submicron resolution. Thus, shaped THz pulses can be achieved from the PLN crystal of which the domain structure coincide with the pulse shape.

Shaped THz pulses are generated via optical rectification in the pre-engineered domain structure of PLN. The generation scheme is illustrated in Fig. 1. The vertical lines in Fig. 1 indicate domain boundaries. The second order nonlinear susceptibility $[\chi^{(2)}]$ of the crystal reverses sign between neighboring domains. When a femtosecond optical pulse propagates through a PLN crystal with the domain structure, a THz nonlinear polarization is generated via optical rectification as illustrated in Fig. 1. Due to the group velocity mismatch between optical and THz waves (the optical and THz indices of refraction are $n_o=2.3$ and $n_t=5.2$, respectively), the optical pulse will lead the THz pulse by the optical pulse duration τ_p after a walk-off length $l_w=c\tau_p/(n_t-n_o)$.[12] If the domain length of the poled nonlinear crystal is comparable to the walk-off length, each domain in the crystal contributes a half cycle to the radiated THz field. Since the length of the half-cycle pulse is proportional to the corresponding domain length, the resulting THz pulse directly maps out the crystal domain structure.

Experimental data have been taken and a numerical simulation was performed for three types of poled $LiNbO_3$ structures. HCP Photonics Corp. fabricated the samples based on our mask design. The poling resolution is about 0.1 μm. Figure 2 shows the diagram of the three domain structures. Black (up) and white (down) indicates the alternating

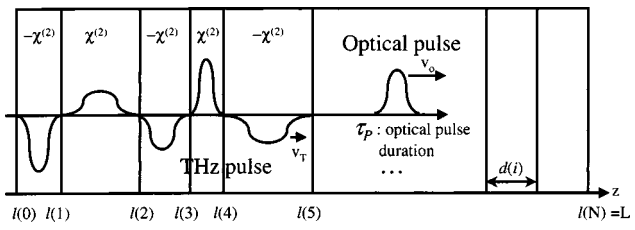

FIG. 1. Schematic diagram of the THz wave form synthesis in a poled nonlinear crystal. The THz wave form coincides with the crystal domain structure.

[a]Electronic mail: leeys@physics.orst.edu

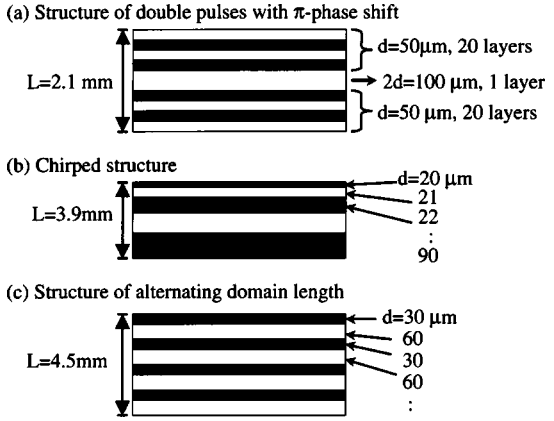

FIG. 2. Diagram of the three types of PLN structures. The cross-sectional size of the crystals is 0.5×5 mm. (a) The structure of double pulses with π-phase shift includes a single domain (100 μm) placed between two sets of 20 domains (50 μm). (b) The domain structure for the chirped pulse includes 71 domains ranging from 20 to 90 μm with 1 μm gradual increment. (c) The structure consists of alternating domains of 30 and 60 μm.

direction of the crystal optic axis. We performed the experiment using 800 nm, 100 fs pulses from a 76 MHz Ti:sapphire oscillator (Coherent Inc., Mira 900F). The femtosecond pulses with 7 nJ pulse energy were focused to a spot of 20 μm diameter in the crystals. We employed electro-optic sampling technique to detect the THz fields.[16] THz radiation was collimated with a pair of off-axis parabolic mirrors and focused into a 1 mm ZnTe crystal for electro-optic detection of the THz field. The excitation beam was modulated at 1 kHz for lock-in signal detection.

The simulation is a solution of the one-dimensional wave equation including the second order nonlinear polarization.[12,13] The local THz field is proportional to the second order time derivative of the second order nonlinear polarization induced by optical rectification. Assuming that a Gaussian optical pump pulse propagates in the z direction, the local THz field per unit length is

$$\varepsilon_L(z,t)=\varepsilon_0\left[\frac{2(z-v_0t)^2}{v_0^2\tau^2}-1\right]\exp\left\{-\frac{(z-v_0t)^2}{v_0^2\tau^2}\right\} \propto \frac{\partial^2 P^{(2)}(z,t)}{\partial t^2}, \tag{1}$$

where τ is optical pulse duration and v_0 is group velocity of the optical pulse in the medium. For given time and position, THz field amplitude is

$$E_{\mathrm{THz}}(z,t) = \int_0^z \pm\varepsilon_L\left[z'-v_0\left(t-\frac{z-z'}{v_t}\right)\right]dz' = \sum_{i=1}^{N}(-1)^{i-1}\int_{l_{i-1}}^{l_i}\varepsilon_L\left[z'-v_0\left(t-\frac{z-z'}{v_t}\right)\right]dz', \tag{2}$$

where L is crystal length, l_i is the position of ith interface, and N is the number of domains. v_t is group velocity of THz wave in the medium. The sign of the local field is determined by the optic axis orientation of the domain. We neglect the dispersion of the optical pulse and the THz wave in the medium.

Figure 3 shows the experimental data and numerical solution of the shaped THz pulses from the PLN crystals. The zero-area double pulse [Figs. 3(1-a, 2-a)] consisting of two pulses with a π-phase shift is generated from a domain structure in which a single domain (100 μm) is placed between two sets of multiple domains (50 μm) [Fig. 2(a)]. The corresponding spectra of the zero-area double pulses [Figs. 3(1-d, 2-d)] clearly show the signature of the interference fringes of two coherent pulses. In Figs. 3(1-b, 2-b), a chirped THz wave form is demonstrated. The domain structure for the chirped pulse includes multiple domains ranging from 20 to 90 μm [Fig. 2(b)]. The broadband spectra are shown in Figs. 3(1-e, 2-e). Figures 3(1-c, 2-c) shows the wave forms from a structure of alternating domain length (30 and 60 μm) [Fig. 2(c)]. Narrow and broad half-cycle pulses appear alternately. Figures 3(1-f, 2-f) show the narrow band spectra corresponding to the 90 μm period. Second harmonic signal appears because of the asymmetric domain structure. The experimental data and simulation results clearly show that shaped THz pulses can be generated in PLN structures and the wave forms mimic the PLN domain structures.

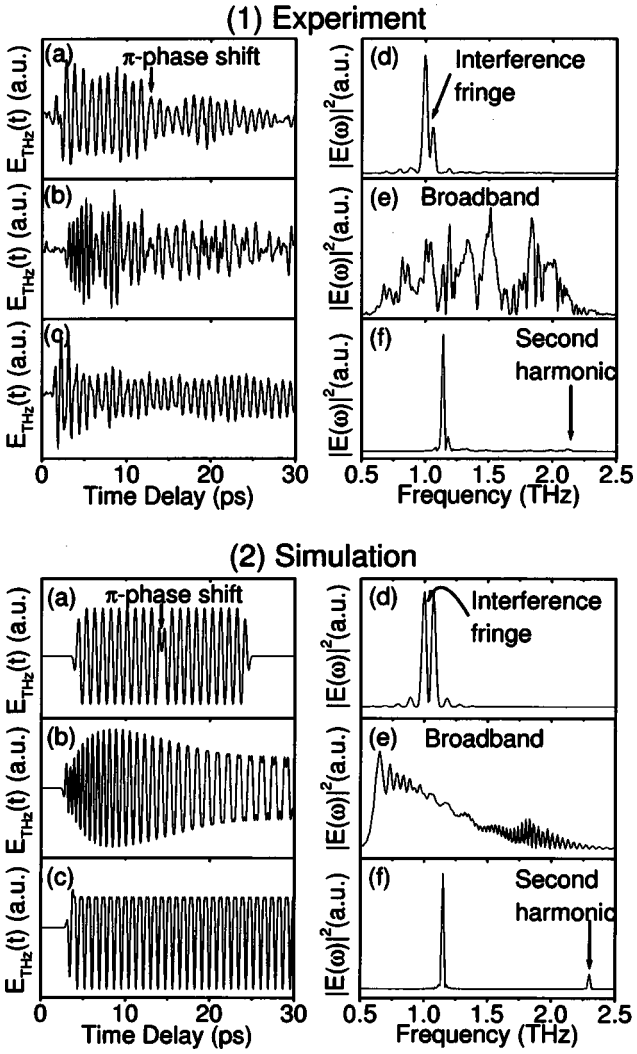

FIG. 3. (1) Experimental data and (2) numerical solution of (a),(d) zero area double, (b),(e) chirped, and (c),(f) alternating THz wave forms and corresponding spectra from poled $LiNbO_3$ structures.

In spite of the good qualitative agreement between experiment and simulation results, there is some quantitative discrepancy. This mainly comes from the oversimplified as-

sumptions in the simulation: the neglect of the dispersion at THz frequency in $LiNbO_3$ crystal and the plane wave approximation. The dielectric function of $LiNbO_3$, actually, is almost constant in wide range of THz frequency.[17] The little dispersion, however, becomes prominent for the propagation distance longer than 1 mm. One prominent feature is that the experimental data decay in time. The main source of the absorption is the low frequency tail of the TO phonon mode at 7.6 THz.[17,18] In Fig. 3(1-a), the second pulse is weaker than the first because of the absorption, thus the interference fringe in the spectrum is asymmetric [Fig. 3(1-d)]. The longer propagation distance of the low frequency component than the high frequency component in Fig. 3(1-b) gives rise to the suppression of the low frequency component in the spectrum [Fig. 3(1-e)]. The second harmonic component is less significant in the experiment [Fig. 3(1-f)] than in the simulation [Fig. 3(2-f)] since the absorption coefficient is larger in high frequency range than in low frequency range. The absorption can be substantially reduced if the crystal temperature is lowered cryogenically.[13] Besides the TO phonon mode at 7.6 THz, additional low-frequency resonances (1.3, 2.4, 3.4, and 4.1 THz)[17,18] have been observed and can contribute the distortion of the THz pulse shape in the experiments. The plane wave approximation (one-dimensional wave equation) is another simplification to cause the discrepancy between the experiment and simulation. The spot size (20 μm) of the optical pump is even smaller than the THz wavelength ($\sim$300 μm), thus the THz wave diffracts very strongly and nonuniformly over the crystal with such a small spot.

We have demonstrated that THz pulse shaping can be achieved in PLN crystals and the THz wave forms correspond to the PLN domain structures. The experiment and simulation results agree well qualitatively. The oversimplifications of the assumption in the simulation are considered as the reasons for the quantitative discrepancy. The exact estimation of THz pulse shape is critical to the precise control of the THz pulse shaping in PLN crystals because the PLN domain structure for required THz pulse shape is to be fabricated before the THz wave generation. In order to obtain an exact wave form of the desired THz pulse, the accurate measurement of the linear dispersion of $LiNbO_3$ in THz range must precede any theoretical estimation. THz time-domain ellipsometry technique can be applied to the measurement of the index of refraction. Also, a more elaborate theory than the one-dimensional wave equation is needed that includes the exact dispersion of $LiNbO_3$ in THz range and expands the dimension of the wave equation. The theory must be capable of inversely solving the nonlinear wave equation. Given the desired THz wave form, it must infer the corresponding domain structures.

The authors are grateful to T. B. Norris for fruitful discussions. The work was supported by the Oregon State University start-up fund.

[1] D. H. Auston, K. P. Cheung, J. A. Valdmanis, and D. A. Kleinman, Phys. Rev. Lett. **53**, 1555 (1984).
[2] K. P. Cheung and D. H. Auston, Phys. Rev. Lett. **55**, 2152 (1985).
[3] L. Xu, X.-C. Zhang, and D. H. Auston, Appl. Phys. Lett. **61**, 1784 (1992).
[4] A. Bonvalet, M. Joffre, J. L. Martin, and A. Migus, Appl. Phys. Lett. **67**, 2907 (1995).
[5] R. Huber, A. Brodschelm, F. Tauser, and A. Leitenstorfer, Appl. Phys. Lett. **76**, 3191 (2000).
[6] H. Harde, S. Keiding, and D. Grischkowsky, Phys. Rev. Lett. **66**, 1834 (1991).
[7] M. van Exter, Ch. Fattinger, and D. Grischkowsky, Opt. Lett. **14**, 1128 (1989).
[8] E. Knoesel, M. Bonn, J. Shan, and T. F. Heinz, Phys. Rev. Lett. **86**, 340 (2001).
[9] C. Rønne, P. Åstrand, and S. R. Keiding, Phys. Rev. Lett. **82**, 2888 (1999).
[10] C. Rønne, K. Jensby, B. J. Loughnane, J. Fourkas, O. F. Nielsen, and S. R. Keiding, J. Chem. Phys. **113**, 3749 (2000).
[11] T. I. Jeon, D. Grischkowsky, A. K. Mukherjee, and R. Menon, Appl. Phys. Lett. **77**, 2452 (2000).
[12] Y.-S. Lee, T. Meade, V. Perlin, H. Winful, T. B. Norris, and A. Galvanauskas, Appl. Phys. Lett. **76**, 2505 (2000).
[13] Y.-S. Lee, T. Meade, M. DeCamp, T. B. Norris, and A. Galvanauskas, Appl. Phys. Lett. **77**, 1244 (2000).
[14] Y.-S. Lee, T. Meade, T. B. Norris, and A. Galvanauskas, Appl. Phys. Lett. **78**, 3583 (2001).
[15] Y.-S. Lee, T. Meade, M. L. Naudeau, T. B. Norris, and A. Galvanauskas, Appl. Phys. Lett. **77**, 2488 (2000).
[16] Q. Wu and X.-C. Zhang, Appl. Phys. Lett. **68**, 1604 (1996).
[17] H. J. Bakker, S. Hunsche, and H. Kurz, Phys. Rev. B **50**, 914 (1994).
[18] U. T. Schwartz and M. Maier, Phys. Rev. B **53**, 5074 (1996).